CHALMERS
UNIVERSITY OF TECHNOLOGY

Impact of Phase Noise on Uplink Cell-Free Massive MIMO OFDM

Citation for the original published paper (version of record):
Wu, Y., Sanguinetti, L., Gustavsson, U. et al (2023). Impact of Phase Noise on Uplink Cell-Free Massive MIMO OFDM. Proceedings - IEEE Global Communications Conference, GLOBECOM: 5829-5834. http://dx.doi.org/10.1109/GLOBECOM54140.2023.10437146

Impact of Phase Noise on Uplink Cell-Free Massive MIMO OFDM

Yibo Wu*†, Luca Sanguinetti‡, Ulf Gustavsson*, Alexandre Graell i Amat†, and Henk Wymeersch†
*Ericsson Research, Gothenburg, Sweden
†Department of Electrical Engineeering, Chalmers University of Technology, Gothenburg, Sweden
‡Dipartimento di Ingegneria dell'Informazione, University of Pisa, Pisa, Italy

***Abstract*—Cell-Free massive MIMO networks provide huge power gains and resolve inter-cell interference by coherent processing over a massive number of distributed instead of co-located antennas in access points (APs). Cost-efficient hardware is preferred but imperfect local oscillators in both APs and users introduce multiplicative phase noise (PN), which affects the phase coherence between APs and users even with centralized processing. In this paper, we first formulate the system model of a PN-impaired uplink Cell-Free massive MIMO orthogonal frequency division multiplexing network, and then propose a PN-aware linear minimum mean square error channel estimator and derive a PN-impaired uplink spectral efficiency expression. Numerical results are used to quantify the spectral efficiency gain of the proposed channel estimator over alternative schemes for different receiving combiners.**

***Index Terms*—Cell-Free massive OFDM MIMO, hardware impairments, phase noise, channel estimation, spectral efficiency.**

I. Introduction

Massive MIMO offers phenomenal received power gains by coherently transmitting a signal over multiple antennas without increasing the transmit power [1]. This coherent transmission can be implemented in two ways, classified by the deployment of antennas: deploying co-located antennas leads to cellular network [2], while deploying distributed antennas over APs leads to cell-free network [3]–[5]. Coherent transmissions in cell-free networks relies on both time and phase synchronization among APs [6]. Even if there is a centralized central processing unit (CPU) that synchronizes all APs, the imperfect LOs at both APs and user equipments (UEs) introduce different PN that varies over time, which unavoidably affects the transmission coherence and reduces the power gain [7]. Using better quality LOs can alleviate the PN problem, while the corresponding hardware cost scales up with up to hundreds of LOs in APs and UEs. Thus, to design an economical and reliable cell-free network, it is important to evaluate the relation of the PN impact and the LO quality.

This work was supported by the Swedish Foundation for Strategic Research (SSF), grant no. ID19-0021, the Gigahertz-ChaseOn Bridge Center at Chalmers in a project financed by Chalmers, Ericsson, and Qamcom, and scholarships from Chalmersska forskningsfonden and S.o.KG. Eliassons minnes- och tilläggsfonder. L. Sanguinetti was partially supported by the Italian Ministry of Education and Research (MUR) in the framework of the FoReLab project (Departments of Excellence), and by the Università di Pisa under the "PRA – Progetti di Ricerca di Ateneo" (Institutional Research Grants) - Project no. PRA 2022-2023-91.

There exist several works investing the PN impact on either cellular or cell-free massive MIMO networks [6]–[12]. However, the vast majority of these works model the PN in a single-carrier fashion, while most modern communication systems utilize OFDM. The loss of orthogonality between OFDM subcarriers in the presence of PN is ignored by the conventional single-carrier models. This may have an impact on the design of the network. For example, it may result into a mismatched channel estimator and a mismatched combining/precoding scheme. The authors in [11] studied the PN impact on the uplink achievable spectral efficiency (SE) in an OFDM system under the assumption of perfect channel state information, while a practical PN-aware channel estimation and the corresponding achievable SE are not studied.

The aim of this paper is to evaluate the impact of PN in the uplink of cell-free OFDM massive MIMO. To this end, we first provide the PN-impaired system model, which correctly models the impact of the time-domain PN on any subcarrier of the received frequency-domain OFDM symbols. The model is then used to derive the PN-aware LMMSE channel estimation scheme and a novel uplink achievable SE considering the intercarrier interference (ICI) caused by the PN. Numerical results are used to evaluate the SE and to show that the proposed channel estimator provides higher SE compared to both PN-aware and PN-unaware estimators stemmed from single-carrier systems.

Notation: Lowercase and uppercase boldface letters, $\boldsymbol{x}$ and $\boldsymbol{X}$, denote column vectors and matrices respectively. The superscripts $^{\mathsf{T}}$, *, $^{\mathsf{H}}$ and † denote transpose, conjugate, conjugate transpose, and pseudo-inverse, respectively. Variables with the check mark $\check{}$, e.g., $\check{x}$, represents that they are in time-domain. The $n \times n$ identity matrix is $\mathbf{I}_n$. We use $\triangleq$ for definitions and $\mathrm{diag}(\boldsymbol{x})$ for a diagonal matrix with $\boldsymbol{x}$ on the diagonal. The expected value of $\boldsymbol{x}$ is denoted by $\mathbb{E}\{\boldsymbol{x}\}$.

II. System Model

We consider a cell-free OFDM network comprising L randomly distributed single-antenna APs, which are connected to a CPU via a fronthaul network and serve K single-antenna UEs. Each OFDM symbol consists of N subcarriers with spacing Δ_f. A cyclic prefix (CP) length of N_{CP} is considered. The signal bandwidth is $W = N\Delta_f$ so that the sampling time is $T_s = 1/W$. The OFDM symbol time is $T = NT_s = 1/\Delta_f$.

A. Block Fading Channel Model

The time-domain channel between UE k and AP l is modeled as a Q-tap finite impulse response filter $\check{\boldsymbol{h}}_{k,l} = [\check{h}_{k,l,0}, \cdots, \check{h}_{k,l,Q-1}]^{\mathsf{T}}$, where the filter length Q is no longer than the multi-path delay spread T_d normalized by the sampling time, i.e., $Q \leq \lceil T_d/T_s \rceil$. The corresponding channel in frequency-domain can be obtained by an N-point discrete Fourier transform (DFT) on $\check{\boldsymbol{h}}_{k,l}$. This yields a correlated channel in the frequency domain. In this paper, we neglect this correlation but assume that the time-frequency resources are divided into coherence blocks where each channel is time-invariant and frequency-flat, considering the standard TDD multicarrier protocol of a canonical massive MIMO network from [2]. As illustrated in Fig. 1, each coherence block has a coherence time $T_c = \tau_c T$ and a coherence bandwidth $W_c = N_c \Delta f$, i.e., τ_c OFDM symbols and N_c subcarriers. In total, the number of coherent *channel uses*, i.e., number of coherent samples, is $W_c T_c = \tau_c N_c$, consisting of τ_p and $(\tau_c N_c - \tau_p)$ channel uses for pilot and data, respectively. Subcarriers in each OFDM symbol are split by $R = \lceil N/N_c \rceil$ coherence blocks, where the subcarrier set in the coherence block $r \in \{1, \cdots, R\}$ is denoted by $\mathcal{R}_r = \{(r-1)N_c, \cdots, rN_c - 1\}$. For an arbitrary coherence block r, the frequency-domain channel between UE k and AP l over subcarrier $n \in \mathcal{R}_r$ is denoted by $h_{k,l,n} \sim \mathcal{N}_{\mathbb{C}}(0, \beta_{k,l})$, where $\beta_{k,l}$ represents the large-scale fading coefficient. Notice that $h_{k,l,n_1} = h_{k,l,n_2}$, for $n_1, n_2 \in \mathcal{R}_r$, while $\mathbb{E}\{h_{k,l,n_1} h_{k,l,n_2}\} = \mathbb{E}\{h_{k_1,l,n} h_{k_2,l,n}\} = 0$, for $n_1, n_2 \notin \mathcal{R}_r$ and $k_1 \neq k_2$.

B. Phase Noise Model

Imperfect LOs at APs and UEs introduce PN. The PN $\check{\phi}_{l,m}^{(\tau)}$ and $\check{\varphi}_{k,m}^{(\tau)}$ from the LOs of AP l and UE k, respectively, at time sample m of OFDM symbol τ, can be modeled as discrete-time Wiener processes [13],

$$\check{\phi}_{l,m}^{(\tau)} = \check{\phi}_{l,m-1}^{(\tau)} + \check{\delta}_m^{\phi}, \ \check{\varphi}_{k,m}^{(\tau)} = \check{\varphi}_{k,m-1}^{(\tau)} + \check{\delta}_m^{\varphi}, \tag{1}$$

where $\check{\delta}_m^{\phi} \sim \mathcal{N}(0, \sigma_\phi^2)$ and $\check{\delta}_n^{\varphi} \sim \mathcal{N}(0, \sigma_\varphi^2)$. The increment variance of the PN process is modeled as $\sigma_i^2 = 4\pi^2 f_c^2 \gamma_i T_{\mathrm{s}}$, for $i \in \{\phi, \varphi\}$, where f_{c} and γ_i denote the carrier frequency and a constant describing the oscillator quality. Note that different APs and UEs may have different quality. The uplink received PN from UE k and AP l at time-domain sample m of OFDM symbol τ is combined as $\check{\theta}_{k,l,m}^{(\tau)} = \check{\phi}_{l,m}^{(\tau)} + \check{\varphi}_{k,m}^{(\tau)}$, and its vector form for the whole OFDM symbol τ is denoted by $\check{\boldsymbol{\theta}}_{k,l}^{(\tau)} = [\check{\theta}_{k,l,0}^{(\tau)}, \cdots, \check{\theta}_{k,l,N-1}^{(\tau)}]^{\mathsf{T}}$. Considering the CP length N_{CP}, the phase noise at the first time-domain sample of $(\tau+1)$-th OFDM symbol can be modeled as $\check{\theta}_{k,l,0}^{(\tau+1)} = \check{\theta}_{k,l,N-1}^{(\tau)} + \check{\delta}^{\mathrm{CP}}$, where $\check{\delta}^{\mathrm{CP}} \sim \mathcal{N}(0, (N_{\mathrm{CP}}+1)(\sigma_\phi^2 + \sigma_\varphi^2))$.

For any OFDM symbol τ, the multiplicative PN $\exp(j\check{\boldsymbol{\theta}}_{k,l}^{(\tau)}) \in \mathbb{C}^N$ in time-domain is equivalent to the convolutional frequency-domain phase-drift vector $\boldsymbol{J}_{k,l}^{(\tau)} \in \mathbb{C}^N$, whose i-th entry $J_{k,l,i}^{(\tau)}$, for $i = -N/2, \cdots, N/2-1$, is obtained by [13]

$$J_{k,l,i}^{(\tau)} = \frac{1}{N} \sum_{n=0}^{N-1} e^{j\theta_{k,l,n}^{(\tau)}} e^{-j2\pi ni/N}. \tag{2}$$

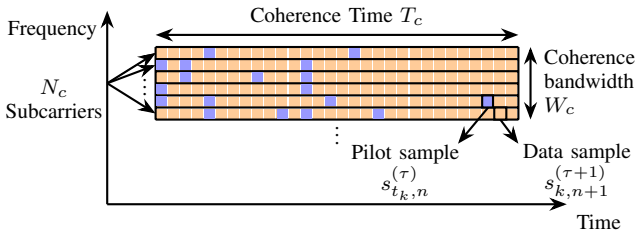

Fig. 1. An example of coherence block r over the time-frequency plane consisting of $\tau_c N_c$ channel uses with an arbitrary pilot distribution.

For $i = 0$, the phase-drift $J_{k,l,0}^{(\tau)} = 1/N \sum_n e^{j\check{\theta}_{k,l,n}^{(\tau)}}$ is known as the common phase error (CPE) [13] since it acts on all subcarriers. The other non-zero phase-drifts $J_{k,l,i}^{(\tau)}$ for $i \neq 0$ lead to ICI. The correlation between $J_{k,l,i_1}^{(\tau_1)}$ and $J_{k,l,i_2}^{(\tau_2)}$ is calculated as [13]

$$\mathbb{E}\{J_{k,l,i_1}^{(\tau_1)} J_{k,l,i_2}^{*(\tau_2)}\} \triangleq B_{i_1,i_2}^{(\tau_1-\tau_2)} = \frac{1}{N^2} \sum_{n_1=0}^{N-1} \sum_{n_2=0}^{N-1} e^{-\frac{\sigma_\varphi^2+\sigma_\phi^2}{2}(|(\tau_1-\tau_2)N+n_1-n_2|)} e^{\frac{-j2\pi(n_1 i_1 - n_2 i_2)}{N}}. \tag{3}$$

C. Uplink Pilot Assignment

We assume the network utilizes a pilot book consisting of τ_p mutually orthogonal τ_p-length frequency-domain pilot sequences, collected into a pilot set $\mathcal{S}_p = \{\boldsymbol{s}_1, \boldsymbol{s}_2, \ldots, \boldsymbol{s}_{\tau_p}\}$, with $\|\boldsymbol{s}_t\|^2 = \tau_p$ and $\boldsymbol{s}_{t_1}^{\mathsf{H}} \boldsymbol{s}_{t_2} = 0$ for $t_1 \neq t_2$. We assume each UE uses the same pilot sequence for all coherence blocks. In each coherence block, the rest of the $(N_c\tau_c - \tau_p)$ channel uses are used for data transmission. When $K > \tau_p$, users have to share pilots, which causes pilot contamination [2]. An arbitrary distribution of the τ_p-length pilot in an coherence block can be implemented, as shown in Fig. 1. For an arbitrary coherence block r, the set of subcarrier and OFDM symbol indices used for pilot transmission is denoted by $\mathcal{N}_p = \{n_1, \cdots, n_{\tau_p}\} \subseteq \mathcal{R}_r$, and $\mathcal{T}_p = \{\tau_1, \cdots, \tau_{\tau_p}\} \subseteq \{1, \cdots, \tau_c\}$, respectively. The set of remaining subcarrier indices for data transmission is denoted by $\mathcal{N}_d = \mathcal{R}_r \backslash \mathcal{N}_p$. We assume all UEs use the same pilot distribution.

UE k is assigned with pilot $\boldsymbol{s}_{t_k} \in \mathbb{C}^{\tau_p}$ from $\mathcal{S}_p$, where we denote the index of the pilot assigned to UE k as $t_k \in \{1, \cdots, \tau_p\}$. UE k distributes its pilot $\boldsymbol{s}_{t_k}$ over pilot subcarriers $n \in \mathcal{N}_p$ and OFDM symbols $\tau \in \mathcal{T}_p$, with each sample denoted by $s_{t_k,n}^{(\tau)}$. The τ-th OFDM symbol of UE k is $\boldsymbol{s}_{t_k}^{(\tau)} \in \mathbb{C}^N$, which consists of both pilot and data samples.

D. Signal Model

For UE k, the i-th time-domain sample of τ-th OFDM symbol is obtained by an IDFT on $\boldsymbol{s}_{t_k}^{(\tau)}$ as $\check{s}_{t_k,i}^{(\tau)} = \frac{1}{\sqrt{N}} \sum_{n=0}^{N-1} s_{t_k,n}^{(\tau)} e^{\frac{j2\pi ni}{N}}$, and its vector form for the whole OFDM symbol τ is denoted by $\check{\boldsymbol{s}}_{t_k}^{(\tau)} \in \mathbb{C}^N$. With the PN $\mathrm{diag}(e^{j\check{\boldsymbol{\theta}}_{k,l}^{(\tau)}})$, the time-domain received signal $\check{\boldsymbol{y}}_l^{(\tau)} \in \mathbb{C}^N$ at AP l for the τ-th OFDM symbol is

$$\check{\boldsymbol{y}}_l^{(\tau)} = \sum_{k=1}^{K} \sqrt{p_k} \mathrm{diag}(e^{j\check{\boldsymbol{\theta}}_{k,l}^{(\tau)}}) (\check{\boldsymbol{h}}_{k,l} \circledast \check{\boldsymbol{s}}_{t_k}^{(\tau)}) + \check{\boldsymbol{\eta}}_l^{(\tau)}, \tag{4}$$

where $p_k \geq 0$ is the transmit power of UE k, $\circledast$ denotes the circular convolution, $\check{\boldsymbol{\eta}}_{k,l}^{(\tau)} \sim \mathcal{N}_{\mathbb{C}}(\mathbf{0}, \sigma^2 \boldsymbol{I}_N)$ denotes the thermal noise. By applying a N-point DFT to both sides of (4), the frequency-domain received signal is

$$\boldsymbol{y}_l^{(\tau)} = \sum_{k=1}^{K} \sqrt{p_k} \boldsymbol{J}_{k,l}^{(\tau)} \circledast (\boldsymbol{h}_{k,l} \odot \boldsymbol{s}_{t_k}^{(\tau)}) + \boldsymbol{\eta}_l^{(\tau)}, \tag{5}$$

where $\odot$ denotes the Hadamard product, the thermal noise follows the same distribution $\boldsymbol{\eta}_l^{(\tau)} \sim \mathcal{N}_{\mathbb{C}}(\mathbf{0}, \sigma^2 \boldsymbol{I}_N)$. The elements of the phase-drift $\boldsymbol{J}_{k,l}^{(\tau)}$ are defined in (2). The frequency-domain sample $y_{l,n}^{(\tau)}$ received over subcarrier n can be decomposed as

$$y_{l,n}^{(\tau)} = \sum_{k=1}^{K} \left(\sqrt{p_k} s_{t_k,n}^{(\tau)} h_{k,l,n}^{(\tau)} + \zeta_{k,l,n}^{(\tau)} \right) + \eta_{l,n}^{(\tau)} \tag{6}$$

where

$$h_{k,l,n}^{(\tau)} \triangleq J_{k,l,0}^{(\tau)} h_{k,l,n} \tag{7}$$

is the effective channel (including the CPE) and

$$\zeta_{k,l,n}^{(\tau)} = \sqrt{p_k} \sum_{\jmath=0, \jmath \neq n}^{N-1} s_{t_k,\jmath}^{(\tau)} J_{k,l,n-\jmath}^{(\tau)} h_{k,l,\jmath} \tag{8}$$

is the ICI component over subcarrier n and OFDM symbol τ. Within an arbitrary coherence block r, the effective channels are the same only for subcarriers in the same OFDM symbol,

$$h_{k,l,n_1}^{(\tau_1)} = h_{k,l,n_2}^{(\tau_1)} \neq h_{k,l,n_1}^{(\tau_2)}, \text{ for } \{n_1, n_2\} \in \mathcal{R}_r, \tau_1 \neq \tau_2.$$

Note that the CPE coefficient $J_{k,l,0}^{(\tau)}$ is the same for all subcarriers of OFDM symbol τ. Other phase error coefficients $\{J_{k,l,i}^{(\tau)}, i \neq n\}$ introduce ICIs on an arbitrary subcarrier n. Note also that the different CPEs break the pilot orthogonality.

Finally, observe that utilizing the time-domain single-carrier PN model to the frequency-domain OFDM system model (6) leads to a mismatched system model as in [6]–[10]. The mismatch disappears only if a single carrier system is utilized, where the single-carrier PN model becomes equivalent in both time and frequency domains, i.e., $J_{k,l,n}^{(\tau)} = J_{k,l,0}^{(\tau)} = e^{j\theta_{k,l,0}^{(\tau)}}$, and the effective channel in [6]–[10] becomes the same as (7).

III. Channel Estimation and Uplink Data Transmission With Phase Noise

We now derive a PN-aware channel estimator and an achievable uplink SE expression in the presence of PN in cell-free massive MIMO networks.

A. Channel Estimation With Phase Noise

From (6) and (7), we see that, although the true channels follow a block fading model, the PN make the effective channel $h_{k,l,n}^{(\tau)}$ change over each OFDM symbol τ. For each coherence block, we need to do the channel estimation for just one subcarrier of each OFDM symbol, instead of estimating the effective channel for every channel use as indicated by the single-carrier channel estimation methods in [7], [8]. We now derive an estimator of the effective channel $h_{k,l,n}^{(\tau)}$ for any subcarrier $n \in \mathcal{R}_r$ and OFDM symbol $\tau \in \{1, \cdots, \tau_c\}$. The conventional minimum mean square error (MMSE) estimation is hard to compute since the received signal and channel are not joint Gaussian distributed due to the PN. Therefore, we derive a LMMSE estimator [14]. In the absence of PN, the LMMSE estimator becomes the optimal MMSE estimator [15] since the received samples and channels are jointly Gaussian.

Lemma 1. *The LMMSE estimate of $h_{k,l,n}^{(\tau)}$ based on $\boldsymbol{y}_l \triangleq [y_{l,n_1}^{(\tau_1)}, \cdots, y_{l,n_{\tau_p}}^{(\tau_p)}]^{\mathsf{T}}$ is*

$$\hat{h}_{k,l,n}^{(\tau)} = \hat{h}_{k,l}^{(\tau)} = \sqrt{p_k} \beta_{k,l} \boldsymbol{s}_{t_k}^{\mathsf{H}} \boldsymbol{B}_{0,0}^{(\tau)} \boldsymbol{\Psi}_l^{-1} \boldsymbol{y}_l. \tag{9}$$

where

$$\boldsymbol{B}_{0,0}^{(\tau)} = \operatorname{diag}\left(\left[B_{0,0}^{(\tau-\tau_1)}, \cdots, B_{0,0}^{(\tau-\tau_p)} \right]^{\mathsf{T}} \right) \tag{10}$$

$$\boldsymbol{\Psi}_l = \sum\nolimits_{k=1}^{K} p_k \beta_{k,l} \boldsymbol{\Phi}_k + \boldsymbol{Z}_l^{ICI} + \sigma^2 \mathbf{I}_{\tau_p} \tag{11}$$

$$[\boldsymbol{\Phi}_k]_{\tau_1,\tau_2} = s_{t_k,n_1}^{(\tau_1)} s_{t_k,n_2}^{*(\tau_2)} B_{0,0}^{(\tau_1-\tau_2)}. \tag{12}$$

Here $B_{i_1,i_2}^{(\tau_1-\tau_2)}$ and $\boldsymbol{Z}_l^{ICI}$ are defined in (3) *and* (25)*.*

Proof. See Appendix A. □

With the LMMSE estimation, the channel estimation $\hat{h}_{k,l,m}^{(\tau)}$ is with zero mean and variance $\epsilon_{k,l,m}^{(\tau)} \triangleq p_k \beta_{k,l}^2 \boldsymbol{s}_{t_k,n}^{\mathsf{H}} \boldsymbol{B}_{0,0}^{(\tau)} \boldsymbol{\Psi}_{l,n}^{-1} \boldsymbol{B}_{0,0}^{\mathsf{H},(\tau)} \boldsymbol{s}_{t_k,n}$, and the channel estimation error $\tilde{h}_{k,l,n}^{(\tau)} \triangleq h_{k,l,n}^{(\tau)} - \hat{h}_{k,l,n}^{(\tau)}$ is with zero mean and variance $c_{k,l,m}^{(\tau)} \triangleq \beta_{k,l} - \epsilon_{k,l,m}^{(\tau)}$.

Remark 1. *The PN-aware LMMSE estimator in* (9) *is different from the one in [6]–[10] as a multi-carrier PN model is considered instead of a single-carrier PN model in the OFDM system model, which leads to different impacts of PN statistics in* (10) *and* (11)*.*

B. Uplink Data Transmission

To meet the scalability requirement of CF massive MIMO, we assume that an arbitrary AP l only serves a subset of UEs [15]. We denote the set of UEs served by AP l by [15]

$$\mathcal{D}_l = \{k : d_{k,l} = 1, k \in \{1, \cdots, K\}\}, \tag{13}$$

where $d_{k,l} \in \{0, 1\}$ defines whether UE k and AP l communicate to each other according to the dynamic cooperation clustering (DCC) framework [16]. For an arbitrary AP l, the cardinality $|\mathcal{D}_l|$ is constant as $K \to \infty$ to satisfy the scalability of a CF massive MIMO network.

For UE k, let $s_{k,n}^{(\tau)} \in \mathbb{C}$ denote the uplink data sample over subcarrier $n \in \mathcal{N}_{\mathrm{d}}$ and OFDM symbol $\tau \in \{1, \cdots, \tau_c\}$ with zero mean and power p_k. The received signals from all APs are collected at the CPU as

$$\boldsymbol{y}_n^{(\tau)} = \sum_{k=1}^{K} \boldsymbol{h}_{k,n}^{(\tau)} s_{k,n}^{(\tau)} + \sum_{k=1}^{K} \boldsymbol{\zeta}_{k,n}^{(\tau)} + \boldsymbol{\eta}_n^{(\tau)}, \tag{15}$$

where the concatenate channel, ICI, and thermal noise between UE k and all L APs over subcarrier n of the τ-th OFDM symbol are denoted as $\boldsymbol{h}_{k,n}^{(\tau)} = [h_{k,1,n}^{(\tau)}, \cdots, h_{k,L,n}^{(\tau)}]^{\mathsf{T}}$, $\boldsymbol{\zeta}_{k,n}^{(\tau)} = [\zeta_{k,1,n}^{(\tau)}, \cdots, \zeta_{k,L,n}^{(\tau)}]^{\mathsf{T}}$, and $\boldsymbol{\eta}_n^{(\tau)} \sim \mathcal{N}_{\mathbb{C}}(\mathbf{0}, \sigma^2 \boldsymbol{I}_L)$. The ICI $\zeta_{k,l,n}^{(\tau)}$ is defined in in (6).

The collective channel estimates and channel estimation error are defined by $\hat{\boldsymbol{h}}_{k,n}^{(\tau)} = [\hat{h}_{k,1,n}^{(\tau)}, \cdots, \hat{h}_{k,L,n}^{(\tau)}]^{\mathsf{T}}$ and $\tilde{\boldsymbol{h}}_{k,n}^{(\tau)} = [\tilde{h}_{k,1,n}^{(\tau)}, \cdots, \tilde{h}_{k,L,n}^{(\tau)}]^{\mathsf{T}}$ with zero

$$\mathrm{SINR}_{k,n}^{(\tau)} = \frac{p_k \left| \mathbb{E}\left\{ \boldsymbol{v}_{k,n}^{\mathsf{H},(\tau)} \boldsymbol{D}_k \boldsymbol{h}_{k,n}^{(\tau)} \right\} \right|^2}{\sum_{i=1}^{K} p_i \mathbb{E}\left\{ \left| \boldsymbol{v}_{k,n}^{\mathsf{H},(\tau)} \boldsymbol{D}_k \boldsymbol{h}_{i,n}^{(\tau)} \right|^2 \right\} - p_k \left| \mathbb{E}\left\{ \boldsymbol{v}_{k,n}^{\mathsf{H},(\tau)} \boldsymbol{D}_k \boldsymbol{h}_{k,n}^{(\tau)} \right\} \right|^2 + \rho_{k,n}^{\mathrm{ICI},(\tau)} + \sigma^2 \mathbb{E}\left\{ \left| \boldsymbol{D}_k \boldsymbol{v}_{k,n}^{\mathsf{H},(\tau)} \right|^2 \right\}} \tag{14}$$

means and variances $\mathrm{diag}([\epsilon_{k,1,n}^{(\tau)}, \cdots, \epsilon_{k,L,n}^{(\tau)}]^{\mathsf{T}})$ and $\boldsymbol{C}_{k,n}^{(\tau)} = \mathrm{diag}([c_{k,1,n}^{(\tau)}, \cdots, c_{k,L,n}^{(\tau)}]^{\mathsf{T}})$, respectively.

According to the DCC network, only a subset of the APs participant in the signal detection. The CPU selects a receive combining scalar $v_{k,l,n}^{(\tau)}$ for an arbitrary UE k and AP l, and completes the estimate of $s_{k,n}^{(\tau)}$ by computing the summation

$$\hat{s}_{k,n}^{(\tau)} = \underbrace{\boldsymbol{v}_{k,n}^{\mathsf{H},(\tau)} \boldsymbol{D}_k \boldsymbol{h}_{k,n}^{(\tau)} s_{k,n}^{(\tau)}}_{\text{Desired signal}} + \underbrace{\sum\nolimits_{i \neq k}^{K} \boldsymbol{v}_{k,n}^{\mathsf{H},(\tau)} \boldsymbol{D}_k \boldsymbol{h}_{i,n}^{(\tau)} s_{i,n}^{(\tau)}}_{\text{Inter-user interference}} + \underbrace{\sum\nolimits_{i=1}^{K} \boldsymbol{v}_{k,n}^{\mathsf{H},(\tau)} \boldsymbol{D}_k \boldsymbol{\zeta}_{i,n}^{(\tau)}}_{\text{ICI}} + \boldsymbol{v}_{k,n}^{\mathsf{H},(\tau)} \boldsymbol{D}_k \boldsymbol{\eta}_n^{(\tau)}, \tag{16}$$

where $\boldsymbol{v}_{k,n}^{(\tau)} = [v_{k,1,n}^{(\tau)}, \cdots, v_{k,L,n}^{(\tau)}]^{\mathsf{T}}$ denotes the collective combining vector and $\boldsymbol{D}_k = \mathrm{diag}([d_{k,1}, \cdots d_{k,L}]^{\mathsf{T}})$ denotes a diagonal matrix.

C. Uplink Spectral Efficiency

The ergodic capacity is unknown for this setup with the PN. We follow the use-and-then-forget (UatF) bound in massive MIMO [2, Th. 4.4] and also in [5], [17], [18] for CF massive MIMO to give an achievable SE expression.

Proposition 1. *An achievable SE of UE k at data subcarrier $n \in \mathcal{N}_d$ is given by*

$$SE_{k,n} = \frac{1}{\tau_c} \sum_{\tau=1}^{\tau_c} \log_2(1 + SINR_{k,n}^{(\tau)}), \tag{17}$$

where $SINR_{k,n}^{(\tau)}$ is the effective signal-to-interference-and-noise ratio (SINR) of UE k over subcarrier n, given in (14) *with the ICI term $\rho_{k,n}^{ICI,(\tau)}$ being defined in* (29).

Proof. See Appendix B. □

Note that the SINR in (17) is different for each OFDM symbol τ because of CPE introduced by the time-domain PN.

The SE expression in (17) can be computed numerically for any combiner $\boldsymbol{v}_{k,n}^{(\tau)}$ using Monte Carlo methods. In the context of cell-free massive MIMO, common combiners are represented by maximum ratio (MR), local-partial MMSE (LP-MMSE), MMSE, and partial MMSE (PMMSE) combinings, given as [15, Eqs. (19),(29), (23), (20)]

$$\boldsymbol{v}_{k,n}^{\mathrm{MR},(\tau)} = \boldsymbol{D}_k \hat{\boldsymbol{h}}_{k,n}^{(\tau)} \tag{18}$$

$$\boldsymbol{v}_{k,l,n}^{\text{LP-MMSE},(\tau)} = p_k \Big(\sum_{i \in \mathcal{D}_l} p_i |\hat{h}_{i,l,n}^{(\tau)}|^2 + c_{i,l,n}^{(\tau)} + \sigma^2 \Big)^{\dagger} \hat{h}_{i,l,n}^{(\tau)} \tag{19}$$

$$\boldsymbol{v}_{k,n}^{\mathrm{PMMSE},(\tau)} = p_k \Big(\sum_{i \in \mathcal{P}_k} p_i \hat{\boldsymbol{H}}_{i,n}^{D,(\tau)} + \boldsymbol{Z}_{i,n}^{\prime(\tau)} \Big)^{\dagger} \boldsymbol{D}_k \hat{\boldsymbol{h}}_{i,n}^{(\tau)} \tag{20}$$

$$\boldsymbol{v}_{k,n}^{\mathrm{MMSE},(\tau)} = p_k \Big(\sum_{i=1}^{K} p_i \hat{\boldsymbol{H}}_{i,n}^{D,(\tau)} + \boldsymbol{Z}_{i,n}^{(\tau)} \Big)^{\dagger} \boldsymbol{D}_k \hat{\boldsymbol{h}}_{i,n}^{(\tau)}, \tag{21}$$

where $\hat{\boldsymbol{H}}_{i,n}^{D,(\tau)} = \boldsymbol{D}_k \hat{\boldsymbol{h}}_{i,n}^{(\tau)} \hat{\boldsymbol{h}}_{i,n}^{\mathsf{H},(\tau)} \boldsymbol{D}_k$, $\mathcal{P}_k = \{i : \boldsymbol{D}_k \boldsymbol{D}_i \neq \boldsymbol{0}_L\}$, $\boldsymbol{Z}_{i,n}^{\prime(\tau)} = \boldsymbol{D}_k \big(\sum_{i \in \mathcal{P}_k}^{K} p_i \boldsymbol{C}_{i,n}^{(\tau)} + \sigma^2 \boldsymbol{I}_L \big) \boldsymbol{D}_k$, and $\boldsymbol{Z}_{i,n}^{(\tau)} = \boldsymbol{D}_k \big(\sum_{i=1}^{K} p_i \boldsymbol{C}_{i,n}^{(\tau)} + \sigma^2 \boldsymbol{I}_L \big) \boldsymbol{D}_k$. We refer to a combining scheme PN-aware or PN-unaware, depending on the usage of PN-aware or PN-unaware channel estimators, respectively.

IV. Numerical Results

Numerical results are now given to show the advantage of the proposed PN-aware LMMSE channel estimator over other estimators in a cell-free OFDM network.

A. Scenario

We consider a simulation scenario where $L = 200$ AP and $K = 10$ UEs are independently and uniformly distributed in a 1×1 km square, all equipped with single-antenna. This approximates an infinitely large network with 200 antennas/km^2 and 10 UEs/km^2. We use the same propagation model as in [15] with spatially correlated fading. We assume that the coherence time and bandwidth are $T_c = 1$ ms and $W_c = 180$ kHz, respectively, which fits an coherence block setup of $N_c = 12$ subcarriers with subcarrier spacing $\Delta f = 15$ kHz and $\tau_c = 15$ OFDM symbols. In total, each coherence block contains 180 samples with $\tau_p = 12$ pilot samples and $(N_c \tau_c - \tau_p) = 168$ data samples. We distribute each pilot sequence to the first subcarrier of $\tau_p = 12$ OFDM symbols, i.e., $\mathcal{N}_p = \{0\}$ and $\mathcal{T}_p = \{1, \cdots, 12\}$. Each OFDM symbol contains $N = 1200$ subcarriers which leads to a signal bandwidth $W = 18$ MHz and symbol time $T_s \approx 5.6 \times 10^{-8}$s. We assume a cost-efficient scenario where all APs and UEs equip low-cost LOs, with the same level but lower quality than that in [7], [8], i.e., $\gamma_\phi = \gamma_\varphi = 4 \times 10^{-17}$, which leads to a PN variance $\sigma_\phi^2 = \sigma_\varphi^2 \approx 3.5 \times 10^{-4}$ by setting $f_c = 2$ GHz.

B. Results and Discussion

Fig. 2 illustrates the relation of the uplink SEs per UE to channel uses in the first coherence block for two combining schemes (MR and MMSE) with the same generative model defined in this paper but three different channel estimators: PN-unaware MMSE [15] (marked by circles), single-carrier PN-aware LMMSE [8] (named by PNA-SC and marked by triangles), and the proposed OFDM PN-aware LMMSE (named by PNA-OFDM and marked by squares). We save space to not show the results of LP-MMSE and PMMSE combiners as they imply similar messages. The ideal case of MR and MMSE combinings with no PN are also shown. We notice that both combining schemes with both PN-aware estimators have substantial SE gains over the same combining schemes with conventional PN-unaware MMSE estimator for channel

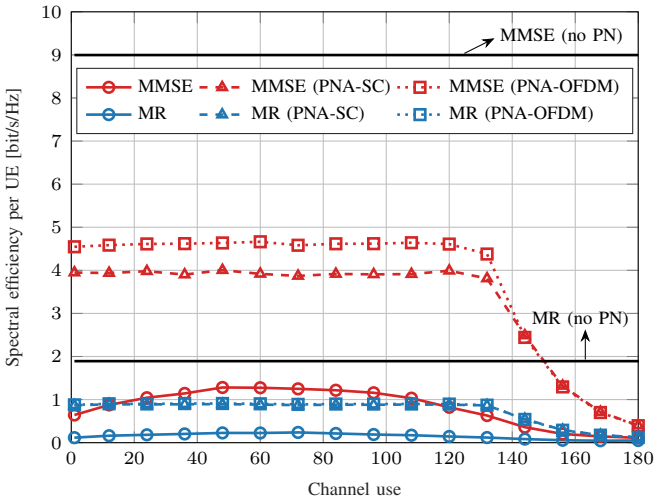

Fig. 2. Uplink SE per UE versus the OFDM symbol τ for two combining schemes with the proposed PN-aware LMMSE, single-carrier PN-aware LMMSE, and PN-unaware MMSE estimators for $\sigma_\phi^2 = \sigma_\varphi^2 = 3.5 \times 10^{-4}$.

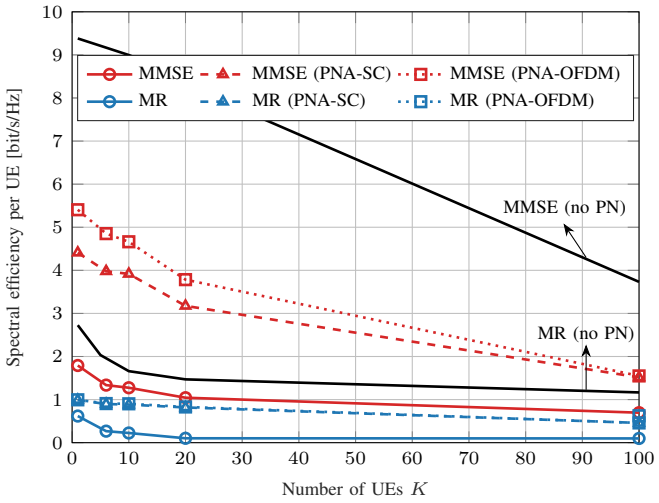

Fig. 3. Uplink SE per UE versus the number of UEs K for two combining schemes with the proposed PN-aware LMMSE, single-carrier PN-aware LMMSE, and PN-unaware MMSE estimators for $\sigma_\phi^2 = \sigma_\varphi^2 = 3.5 \times 10^{-4}$.

uses within the $\tau_p = 12$ pilot OFDM symbols, i.e., channel use ≤ 144, while the SEs drop quickly as the channel use > 144, where the channel aging effects caused by the PN become stronger because the chosen pilot distribution has no pilot samples for OFDM symbol $\tau > \tau_p$. The proposed PN-aware LMMSE estimator performs better than the single-carrier PN-aware LMMSE, especially for the MMSE combiner. This SE gap shows that a mismatched system model as in [6]–[10] ignoring CPEs and ICIs can deteriorate the performance substantially. It is interesting to see only the combining schemes with the PN-unaware estimator have a convex shape, i.e., SEs are better in the middle than the beginning and the end. This can be explained that the PN-aware estimator gives different weights for pilot samples in different OFDM symbols, i.e., $\boldsymbol{B}_{0,0}^{(\tau)}$ in (10), while the PN-unaware MMSE estimator gives the same weights, which happen to fit better for channel uses around $(\tau_p N_c)/2 = 72$.

Fixing the same setup as in Fig. 2 but varying the number of UEs K, we evaluate the corresponding SEs at channel use 60 in Fig. 3. We notice that all SEs decrease as K grows because both the ICI and inter-user interference caused by the PN increase with K as we indicate in Section II-C. The MMSE combining with the proposed PN-aware LMMSE estimator performs the best but eventually degrades to the same as the MMSE (Aware-SC) combining due to strong pilot contamination.

V. Conclusion

In this paper, we derived a signal model of PN-impaired cell-free massive MIMO OFDM networks and proposed a novel PN-aware LMMSE channel estimator, which estimates any aging channel in the coherence block caused by the PN. We derived a new uplink achievable SE expression considering the ICI from all UEs. Numerical results demonstrate the advantage of the proposed PN-aware LMMSE estimator over both PN-unaware and a single-carrier PN-aware estimators for different receiving schemes.

Appendix A
Proof of Lemma 1

The general expression for the LMMSE estimator is [14] $\hat{h}_{k,l,n}^{(\tau)} = \mathbb{E}\{h_{k,l,n}^{(\tau)} \boldsymbol{y}_l^{\mathsf{H}}\} \big(\mathbb{E}\{\boldsymbol{y}_l \boldsymbol{y}_l^{\mathsf{H}}\}\big)^{-1} \boldsymbol{y}_l$, where we have

$$\begin{aligned}\mathbb{E}\{h_{k,l,n}^{(\tau)} \boldsymbol{y}_l^{\mathsf{H}}\} &= \sqrt{p_k}\beta_{k,l} \times \\ &\quad \big[s_{t_k,n_1}^{*(\tau_1)} \mathbb{E}\{J_{k,l,0}^{(\tau)} J_{k,l,0}^{*(\tau_1)}\}, \cdots, s_{t_k,n_{\tau_p}}^{*(\tau_p)} \mathbb{E}\{J_{k,l,0}^{(\tau)} J_{k,l,0}^{*(\tau_p)}\}\big] \\ &= \sqrt{p_k}\beta_{k,l} \boldsymbol{s}_{t_k}^{\mathsf{H}} \boldsymbol{B}_{0,0}^{(\tau)}, \end{aligned} \tag{22}$$

where $\boldsymbol{B}_{0,0}^{(\tau)} = \mathrm{diag}[\mathbb{E}\{J_{k,l,0}^{(\tau)} J_{k,l,0}^{*(\tau_1)}\}, \cdots, \mathbb{E}\{J_{k,l,0}^{(\tau)} J_{k,l,0}^{*(\tau_p)}\}]$ and its τ' element $B_{0,0}^{(\tau-\tau')} \triangleq \mathbb{E}\{J_{k,l,0}^{(\tau)} J_{k,l,0}^{*(\tau')}\}$ is calculated following (3).

Furthermore, we have

$$\begin{aligned}&\mathbb{E}\left\{\boldsymbol{y}_l \boldsymbol{y}_l^{\mathsf{H}}\right\} = \sigma^2 \boldsymbol{I}_{\tau_p} \\ &+ \mathbb{E}\Big\{ \sum_{k=1}^{K} \sqrt{p_k} \big[s_{t_k,n_1}^{(\tau_1)} J_{k,l,0}^{(\tau_1)}, \cdots, s_{t_k,n_{\tau_p}}^{(\tau_p)} J_{k,l,0}^{(\tau_p)}\big]^{\mathsf{T}} h_{k,l,n} \\ &\quad \times h_{k,l,n}^{*} \sqrt{p_k} \big[s_{t_k,n_1}^{(\tau_1)} J_{k,l,0}^{*(\tau_1)}, \cdots, s_{t_k,n_{\tau_p}}^{(\tau_p)} J_{k,l,0}^{*(\tau_p)}\big] \Big\} \\ &+ \mathbb{E}\Big\{ \underbrace{\Big[\sum_{k=1}^{K} \zeta_{k,l,n_1}^{(\tau_1)}, \cdots, \sum_{k=1}^{K} \zeta_{k,l,n_{\tau_p}}^{(\tau_p)}\Big]^{\mathsf{T}}}_{\triangleq \boldsymbol{\zeta}_{k,l}} \boldsymbol{\zeta}_{k,l}^{\mathsf{H}} \Big\} \\ &= \underbrace{\sum_{k=1}^{K} p_k \beta_{k,l} \boldsymbol{\Phi}_k + \boldsymbol{Z}_l^{\mathrm{ICI}}}_{\triangleq \boldsymbol{\Psi}_l} + \sigma^2 \boldsymbol{I}_{\tau_p}, \end{aligned} \tag{23}$$

where the (τ_1, τ_2) element of $\boldsymbol{\Phi}_k \in \mathbb{C}^{\tau_p \times \tau_p}$ is

$$[\boldsymbol{\Phi}_k]_{\tau_1,\tau_2} = s_{t_k,n_1}^{(\tau_1)} s_{t_k,n_2}^{*(\tau_2)} B_{0,0}^{(\tau_1-\tau_2)}. \tag{24}$$

The (τ_1, τ_2) element of the ICI component $\boldsymbol{Z}_l^{\mathrm{ICI}} \in \mathbb{C}^{\tau_p \times \tau_p}$ is

$$\begin{aligned}&[\boldsymbol{Z}_l^{\mathrm{ICI}}]_{\tau_1,\tau_2} \\ &= \mathbb{E}\Big\{ \sum_{k=1}^{K} \zeta_{k,l,n_1}^{(\tau_1)} \sum_{k'=1}^{K} \zeta_{k',l,n_2}^{*(\tau_2)} \Big\} = \sum_{k=1}^{K} \mathbb{E}\left\{ \zeta_{k,l,n_1}^{(\tau_1)} \zeta_{k,l,n_2}^{*(\tau_2)} \right\} \\ &= \sum_{k=1}^{K} p_k \beta_{k,l} \sum_{j_1 \neq n_1}^{N-1} \sum_{j_2 \neq n_2}^{N-1} \mathbb{E}\{ s_{t_k,j_1}^{(\tau_1)} s_{t_k,j_2}^{*(\tau_2)} J_{k,l,n_1-j_1}^{(\tau_1)} J_{k,l,n_2-j_2}^{*(\tau_2)} \} \end{aligned}$$

$$= \sum_{k=1}^{K} p_k \beta_{k,l} \Big(\sum_{\substack{j_1 \in \mathcal{N}_p \\ j_1 \neq n_1}}^{N-1} \sum_{\substack{j_2 \in \mathcal{N}_p \\ j_2 \neq n_2}}^{N-1} s_{t_k,j_1}^{(\tau_1)} s_{t_k,j_2}^{*(\tau_2)} B_{n_1-j_1,n_2-j_2}^{(\tau_1-\tau_2)} + \sum_{\substack{j_1 \in \mathcal{N}_d \\ j_1 \neq n_1}}^{N-1} \sum_{\substack{j_2 \in \mathcal{N}_d \\ j_2 \neq n_2}}^{N-1} B_{n_1-j_1,n_2-j_2}^{(\tau_1-\tau_2)} \Big), \quad (25)$$

where the correlation term $B_{n_1-j_1,n_2-j_2}^{(\tau_1-\tau_2)}$ is calculated following (3).

Appendix B
Proof of Proposition 1

Since the effective channels vary with each OFDM symbol τ, we follow the reference [5, Theorem 4.4] using the UatF bound to obtain an achievable SE for data subcarrier $n \in \mathcal{N}_d$ at OFDM symbol $\tau \in \{1, \cdots, \tau_c\}$. These achievable SEs are averaged over all τ_c OFDM symbols to obtain (17).

Specifically, by adding and subtracting the average effective channel $\mathbb{E}\left\{ \boldsymbol{v}_{k,n}^{\mathsf{H},(\tau)} \boldsymbol{D}_k \boldsymbol{h}_{k,n}^{(\tau)} \right\}$, (16) is rewritten as

$$\hat{s}_{k,n}^{(\tau)} = \mathbb{E}\left\{ \boldsymbol{v}_{k,n}^{\mathsf{H},(\tau)} \boldsymbol{D}_k \boldsymbol{h}_{k,n}^{(\tau)} \right\} s_{k,n}^{(\tau)} + \nu_{k,n}^{(\tau)}, \quad (26)$$

where the interference term is

$$\nu_{k,n}^{(\tau)} = \left(\boldsymbol{v}_{k,n}^{\mathsf{H},(\tau)} \boldsymbol{D}_k \boldsymbol{h}_{k,n}^{(\tau)} - \mathbb{E}\left\{ \boldsymbol{v}_{k,n}^{\mathsf{H},(\tau)} \boldsymbol{D}_k \boldsymbol{h}_{k,n}^{(\tau)} \right\} \right) s_{k,n}^{(\tau)} + \quad (27)$$
$$\sum_{\substack{i=1 \\ i \neq k}}^{K} \boldsymbol{v}_{k,n}^{\mathsf{H},(\tau)} \boldsymbol{D}_k \boldsymbol{h}_{i,n}^{(\tau)} s_{i,n}^{(\tau)} + \sum_{i=1}^{K} \boldsymbol{v}_{k,n}^{\mathsf{H},(\tau)} \boldsymbol{D}_k \boldsymbol{\zeta}_{i,n}^{(\tau)} + \boldsymbol{v}_{k,n}^{\mathsf{H},(\tau)} \boldsymbol{D}_k \boldsymbol{\eta}_n^{(\tau)}.$$

This can be viewed as a deterministic channel with a gain $\mathbb{E}\{\boldsymbol{v}_{k,n}^{\mathsf{H},(\tau)} \boldsymbol{D}_k \boldsymbol{h}_{k,n}^{(\tau)}\}$ and additive interference plus noise term $\nu_{k,n}^{(\tau)}$ that has zero mean. Note that $\nu_{k,n}^{(\tau)}$ is uncorrelated with the desired signal $s_{k,n}^{(\tau)}$ due to the independence between each of the zero-mean symbols $s_{k,n}^{(\tau)}$, i.e., $\mathbb{E}\{s_{i,n}^{(\tau)} s_{j,n}^{(\tau)}\} = \mathbb{E}\{s_{i,n}^{(\tau)} s_{i,j}^{(\tau)}\} = 0$ for $n, j \in \mathcal{N}_d$. The denominator of the SINR in (14) is obtained by

$$\mathbb{E}\{|\nu_{k,n}^{(\tau)}|^2\} = \sum\nolimits_{i=1}^{K} p_i \mathbb{E}\left\{ \left| \boldsymbol{v}_{k,n}^{\mathsf{H},(\tau)} \boldsymbol{D}_k \boldsymbol{h}_{i,n}^{(\tau)} \right|^2 \right\} + \rho_{k,n}^{\text{ICI},(\tau)} - p_k \left| \mathbb{E}\left\{ \boldsymbol{v}_{k,n}^{\mathsf{H},(\tau)} \boldsymbol{D}_k \boldsymbol{h}_{k,n}^{(\tau)} \right\} \right|^2 + \sigma^2 \mathbb{E}\left\{ \left| \boldsymbol{v}_{k,n}^{(\tau)} \boldsymbol{D}_k \right|^2 \right\}. \quad (28)$$

Here, the ICI term $\rho_{k,n}^{\text{ICI},(\tau)}$ is computed as

$$\rho_{k,n}^{\text{ICI},(\tau)} = \sum\nolimits_{i=1}^{K} \mathbb{E}\left\{ \boldsymbol{v}_{k,n}^{\mathsf{H},(\tau)} \boldsymbol{D}_k \boldsymbol{\zeta}_{i,n}^{(\tau)} \boldsymbol{\zeta}_{i,n}^{\mathsf{H},(\tau)} \boldsymbol{D}_k \boldsymbol{v}_{k,n}^{(\tau)} \right\} = \sum\nolimits_{i=1}^{K} \mathbb{E}\left\{ \boldsymbol{v}_{k,n}^{\mathsf{H},(\tau)} \boldsymbol{D}_k \text{diag}(\boldsymbol{\lambda}_{i,n}^{(\tau)}) \boldsymbol{D}_k \boldsymbol{v}_{k,n}^{(\tau)} \right\}, \quad (29)$$

where the l-th element of the ICI power $\boldsymbol{\lambda}_{i,n}^{(\tau)} \in \mathbb{C}^L$ is computed as

$$\lambda_{i,n,l}^{(\tau)} = \sum\nolimits_{j \neq n}^{N-1} \mathbb{E}\{|s_{i,j}^{(\tau)}|^2\} \mathbb{E}\{|h_{i,l,j}|^2\} \mathbb{E}\{|J_{i,l,n-j}^{(\tau)}|^2\} = p_i \beta_{i,l} \sum\nolimits_{j \neq n}^{N-1} B_{n-j,n-j}^{(0)} = p_i \beta_{i,l} (1 - B_{0,0}^{(0)}), \quad (30)$$

where we view the unknown channels over subcarriers other than n as random variables instead of realizations to reduce computation complexity. In the ideal case of no PN, $\lambda_{i,n,l}^{(\tau)} = 0$ and $\rho_{k,n}^{\text{ICI},(\tau)} = 0$, which turns the SINR and SE expressions in (14) and (17) to be the same as in [15].

References

[1] E. Björnson, E. G. Larsson, and T. L. Marzetta, "Massive MIMO: Ten myths and one critical question," *IEEE Commun. Mag.*, vol. 54, no. 2, pp. 114–123, Feb. 2016.

[2] E. Björnson, J. Hoydis, L. Sanguinetti *et al.*, "Massive MIMO networks: Spectral, energy, and hardware efficiency," *Foundations and Trends® Signal Process.*, vol. 11, no. 3-4, pp. 154–655, 2017.

[3] E. Nayebi, A. Ashikhmin, T. L. Marzetta, H. Yang, and B. D. Rao, "Precoding and power optimization in cell-free massive MIMO systems," *IEEE Trans. Wireless Commun.*, vol. 16, no. 7, pp. 4445–4459, May. 2017.

[4] H. Q. Ngo, A. Ashikhmin, H. Yang, E. G. Larsson, and T. L. Marzetta, "Cell-free massive MIMO versus small cells," *IEEE Trans. Wireless Commun.*, vol. 16, no. 3, pp. 1834–1850, Jan. 2017.

[5] Ö. T. Demir, E. Björnson, L. Sanguinetti *et al.*, "Foundations of user-centric cell-free massive MIMO," *Foundations and Trends® Signal Process.*, vol. 14, no. 3-4, pp. 162–472, 2021.

[6] J. Zheng, J. Zhang, J. Cheng, V. C. Leung, D. W. K. Ng, and B. Ai, "Asynchronous Cell-Free massive MIMO with rate-splitting," *IEEE J. Sel. Areas Commun.*, Jan, 2023.

[7] E. Björnson, M. Matthaiou, and M. Debbah, "Massive MIMO with non-ideal arbitrary arrays: Hardware scaling laws and circuit-aware design," *IEEE Trans. Wireless Commun.*, vol. 14, no. 8, pp. 4353–4368, Apr. 2015.

[8] A. Papazafeiropoulos, E. Björnson, P. Kourtessis, S. Chatzinotas, and J. M. Senior, "Scalable cell-free massive MIMO systems: Impact of hardware impairments," *IEEE Trans. Veh. Technol.*, vol. 70, no. 10, pp. 9701–9715, Sep. 2021.

[9] S.-N. Jin, D.-W. Yue, and H. H. Nguyen, "Spectral efficiency of a frequency-selective cell-free massive MIMO system with phase noise," *IEEE Wireless Commun. Lett.*, vol. 10, no. 3, pp. 483–487, Nov. 2020.

[10] Ö. Özdogan, E. Björnson, and J. Zhang, "Performance of cell-free massive MIMO with Rician fading and phase shifts," *IEEE Trans. Wireless Commun.*, vol. 18, no. 11, pp. 5299–5315, Aug. 2019.

[11] A. Pitarokoilis, E. Björnson, and E. G. Larsson, "Performance of the massive MIMO uplink with OFDM and phase noise," *IEEE Commun. Lett.*, vol. 20, no. 8, pp. 1595–1598, Jun. 2016.

[12] J. Zheng, J. Zhang, E. Björnson, Z. Li, and B. Ai, "Cell-free massive MIMO-OFDM for high-speed train communications," *IEEE J. Sel. Areas Commun.*, vol. 40, no. 10, pp. 2823–2839, Aug. 2022.

[13] D. Petrovic, W. Rave, and G. Fettweis, "Effects of phase noise on OFDM systems with and without PLL: Characterization and compensation," *IEEE Trans. Commun.*, vol. 55, no. 8, pp. 1607–1616, Aug. 2007.

[14] S. M. Kay, *Fundamentals of statistical signal processing: estimation theory*. Prentice-Hall, Inc., 1993.

[15] E. Björnson and L. Sanguinetti, "Scalable cell-free massive MIMO systems," *IEEE Trans. Commun.*, vol. 68, no. 7, pp. 4247–4261, Apr. 2020.

[16] E. Bjornson, N. Jalden, M. Bengtsson, and B. Ottersten, "Optimality properties, distributed strategies, and measurement-based evaluation of coordinated multicell OFDMA transmission," *IEEE Trans. Signal Process.*, vol. 59, no. 12, pp. 6086–6101, Aug. 2011.

[17] E. Nayebi, A. Ashikhmin, T. L. Marzetta, and B. D. Rao, "Performance of cell-free massive MIMO systems with MMSE and LSFD receivers," in *Asilomar Conf. Signals Syst. Comput.*, Mar. 2016, pp. 203–207.

[18] M. Bashar, K. Cumanan, A. G. Burr, M. Debbah, and H. Q. Ngo, "On the uplink max–min SINR of cell-free massive MIMO systems," *IEEE Trans. Wireless Commun.*, vol. 18, no. 4, pp. 2021–2036, Jan. 2019.